Applied Catalysis A: General 480 (2014) 50–57

Contents lists available at ScienceDirect

Applied Catalysis A: General

journal homepage: www.elsevier.com/locate/apcata

Effective one-step reduction of Pt/alumina–carbon catalysts for asymmetric hydrogenation of α-ketoesters

Xueqin Zhang*, Qiang Li, Meitian Xiao, Yongjun Liu

College of Chemical Engineering, Huaqiao University, Xiamen, Fujian, 361021, PR China

ARTICLE INFO

Article history:
Received 9 February 2014
Received in revised form 10 April 2014
Accepted 16 April 2014
Available online 24 April 2014

1. Introduction

Asymmetric hydrogenation of activated ketones, using heterogeneous chiral catalysts, plays a key role in the production of fine chemicals [1]. Since the original discovery of Pt-Cinchona system by Orito and co-workers [2,3], the asymmetric hydrogenation of α-ketoesters over cinchonidine(CD)-modified Pt supported catalysts have been studied extensively [4–14]. Particular attention is given to the supports of Pt nanoparticles. Al_2O_3 [4–8], zeolite [15,16], SiO_2 [17], SWNTs [18], MCM-41 [19], CMK-type mesoporous carbon [20,21], FDU-type mesopolymer [22], ionic liquid [23] and carbon nanotubes (CNTs) [24] are considered as suitable supports, furnishing medium to good enantioselectivity. And Al_2O_3 supported Pt catalysts are proved to be the best catalyst for the asymmetric hydrogenation of α-ketoesters. However, the hydrogenation of the aromatic part of CD [25,26] and the intrinsic drawback of Al_2O_3 with inferior stability in acetic acid [27,28] limits the reusability of CD-modified Pt/Al_2O_3 catalyst system, while acetic acid is proved to be one of the best solvents in the asymmetric hydrogenation of α-functionalized ketones on the CD-modified Pt supported catalysts [6,28,29]. In comparison with Pt/Al_2O_3, FDU-type mesopolymer supported Pt catalysts show moderate enantioselectivity but long-term stability by adding modifier after each reaction cycle [22,30].

For the drawbacks of the single-component materials supported catalysts, alumina–X (X represents a kind of material) composites have attracted attention of catalytic chemists gradually. Wang et al. [31] incorporated SBA-15 with alumina (Al_2O_3-SBA-15) by solvent-free solid-state grinding method and the obtained CD-modified Pt/Al_2O_3-SBA-15 catalyst furnished 93.4% ee value in the asymmetric hydrogenation of ethyl pyruvate. Nevertheless, the catalytic property of Pt/Al_2O_3-FDU-14 was in moderate level and this may due to the weak interaction between alumina and FDU-14 [32]. Interestingly, Böttcher and co-workers [33] observed high enantioselectivity (ee up to 94.1%) in the enantioselective hydrogenation of ethyl pyruvate when aluminized fumed silica were used as supports for Pt nanoparticles, CD as modifier. However, all the work about these alumina–X composites supported Pt catalysts was not involved in reusability of relative catalysts.

Pt supported catalysts are commonly prepared by impregnation of supports with chlorine containing platinum precursor and the presence of chlorines limits the aggregation of Pt to obtain high dispersed nanoparticles [5,8]. However, the residual chlorine originating from the chlorine containing precursor hinders the adsorption of reactant and poisons the active metal sites [34,35]. Generally, the residual chlorine cannot be totally removed from the surface by direct reduction in hydrogen [35,36]. The most common reduction method of Cl-containing platinum catalyst precursors is liquid phase reduction, which includes the follow three steps: (a) calcination in air or vacuum; (b) reduction by the aqueous solution of NaCOOH and washing by ionized water; (c) pretreatment before use [5,20–22,24,29,31,37]. The procedures of calcination and aqueous reduction can remove the surface residual chlorines. The pretreatment of the catalyst can be carried out by high temperature [8,38] or sonication [39–41]. Both two pretreatment methods affect the Pt particle size and the surface adsorption of cinchonidine, which can induce asymmetric sites on the catalyst surface and plays an important role in achieving high ee values [13,42,43]. Nevertheless, this traditional multi-steps liquid reduction method is complicated and the hydro-thermal treatment of the catalyst during the aqueous reduction results in Pt loss and structure destruction of the catalyst.

Lately, our group incorporated alumina with mesoporous carbon by chelate-assisted co-assembly method [44]. The Al_2O_3–mesoporous carbon (Al_2O_3–MC) composites were proved

* Corresponding author. Tel.: +86 0592 6162285; fax: +86 0592 6162300.
E-mail address: xqzhang2009@hqu.edu.cn (X. Zhang).

http://dx.doi.org/10.1016/j.apcata.2014.04.031
0926-860X/

to be favorable for high Pt dispersion and the resulting Pt supported catalyst modified with CD showed excellent catalytic performance in the asymmetric hydrogenation of ethyl 2-oxo-4-phenylbutyrate (EOPB). In the further exploration, we found that reduction method played a vital role in the catalytic performance of these Pt/Al_2O_3–MC catalysts and the residual chlorine on the catalyst surface could be removed by one-step reduction in hydrogen. Herein, we mainly focus on uncovering the superiorities of the one-step reduction by using various characterization methods. Additionally, the reusability of Pt/Al_2O_3–MC in the asymmetric hydrogenation of ethyl pyruvate is also studied.

2. Experimental

2.1. Catalyst preparation

The mesoporous carbon incorporated with 15 wt% alumina was prepared according to Ref. [44]. The obtained 15 wt% Al_2O_3–MC composites was denoted as 15AM. The 5 wt% Pt/15AM was prepared by impregnation method. 15AM composites were impregnated with an aqueous solution of platinum precursor (H_2PtCl_6) and stirred for 5 h. Then the mixture was evaporated to remove the excess water, followed by drying at 373 K for 12 h. One portion of the catalyst precursor was reduced in an aqueous solution of sodium formate at 368 K for 1 h, then the mixture was washed by deionized water for three times and dried at 373 K for 12 h. Before use, the catalyst was pretreated at different temperature in a hydrogen flow. The other portion was directly reduced in a hydrogen flow. The obtained catalysts were denoted as Pt/15AM-SF-T, where SF is the abbreviation of sodium formate, and *T* stands for the temperature at which the catalyst precursor was reduced. The description without SF stands for the catalyst directly reduced in a hydrogen flow. As a comparison, Al_2O_3 supported Pt catalyst was prepared. A portion of Pt/Al_2O_3 precursor was reduced directly at 600 °C in hydrogen and denoted as Pt/Al_2O_3-600. The other portion Pt/Al_2O_3 precursor was reduced according to Ref. [29] and the obtained catalyst was denoted as Pt/Al_2O_3-SF-400.

2.2. Characterization

Powder X-ray diffraction (XRD) patterns were collected on a Panalytical X'Pert-Pro powder X-ray diffractometer using Cu Kα radiation (40 kV, 40 mA). The low and wide scan ranges were 0.5–5° and 20–90°, respectively. N_2 adsorption–desorption isotherms were recorded on a Micrometitics ASAP 2020M+C analyzer at −196 °C. The BET method was adopted to calculate the special surface areas using adsorption data in a relative pressure range from 0.05 to 0.25. The pore size distributions were derived from the adsorption branches of isotherms using the BJH model. Transmission electronic microscopy (TEM) images were taken on a HITACHI H-7650 electronic microscope with an accelerating voltage of 100 kV.

The XPS spectra were recorded on a Physical Electronics PHI Quantum-2000 spectrometer with a monochromatized AlKα source ($h\nu$ = 1486.6 eV). The measurements were performed at room temperature in a high vacuum of 2×10^{-7} Pa.

The exact Pt contents of the catalysts were measured with an Optima 7000 DV inductively coupled plasma optical emission spectroscopy (ICP-OES). Before ICP-OES measurement, the samples were calcined at 873 K for 1 h in air and then dissolved in aqua regia.

2.3. Catalytic testing

The catalytic performance of Pt/15AM-SF-T for asymmetric hydrogenation of EOPB to (*R*)-(+)-ethyl 2-hydroxy-4-phenylbutyrate ((*R*)-(+)-EHPB) were evaluated in a 100 mL stainless-steel stirred pressure reactor at room temperature. Pt/15AM catalyst (100 mg), CD (10 mg), ethyl pyruvate (2 mL) or EOPB (1 mL), solvent (25 mL) and H_2 (5 MPa) were used for the reaction. The reaction was terminated after a while and then the products were analyzed by gas chromatography (Agilent 6890) equipped with capillary chiral column (CP-ChiraSil-DEX CB 25 m × 0.25 mm × 0.25 μm, Agilent). The optical yield was expressed as ee value: ee (%) = ([*R*] − [*S*])/([*R*] + [*S*]) × 100.

After the reaction, the catalyst was separated and washed with fresh acetic acid. Fresh reactant, CD and acetic acid were added to the reactor together with the recovered catalyst to carry out the next cycle reaction.

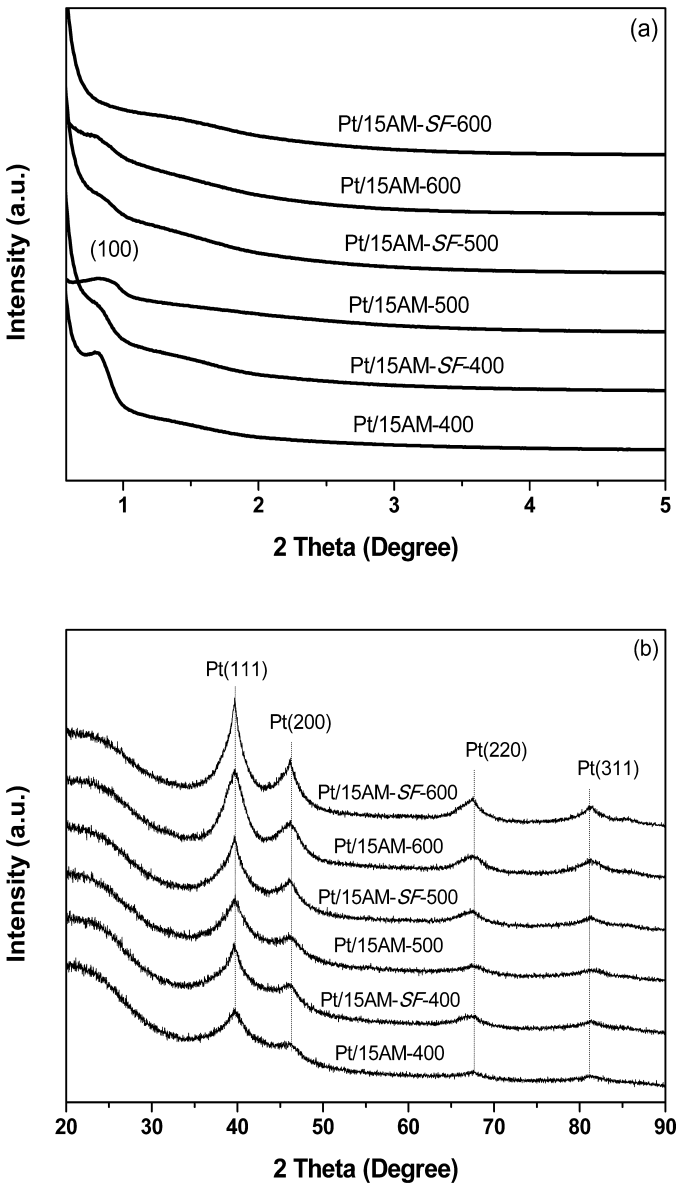

Fig. 1. Low-angle (a) and wide-angle (b) XRD patterns of Pt/15AM-T and Pt/15AM-SF-T catalysts.

3. Results and discussion

3.1. XRD

Fig. 1a shows the low-angle XRD patterns of Pt/15AM-T and Pt/15AM-SF-T catalysts. The diffraction peaks at 2θ = 0.6–1.0°

Table 1
Relevant parameters of Pt/15AM and Pt/Al_2O_3 reduced by different methods.

Entry	Sample	S_{BET} (m^2/g)	V_t (cm^3/g)	D_p (nm)	D_{pt} (nm)[a]	Pt content (wt %)[b]
1	Pt/15AM-400	421	0.29	5.6	3.8	4.9
2	Pt/15AM-SF-400	527	0.33	4.8	4.8	4.3
3	Pt/15AM-500	650	0.47	5.6	4.3	5.5
4	Pt/15AM-SF-500	751	0.54	4.8	6.4	4.9
5	Pt/15AM-600	704	0.70	5.6	6.1	6.9
6	Pt/15AM-SF-600	866	0.82	4.8	8.1	6.0
7	Pt/Al_2O_3-600	170	0.40	6.1	3.0	4.8
8	Pt/Al_2O_3-SF-400	193	0.42	6.8	3.1	3.8

[a] Average Pt particle sizes were measured by TEM.
[b] Exact Pt contents were measured by ICP-OES.

can be indexed to the (1 0 0) reflection of 2-D P6mm hexagonal mesostructure [45]. Along with reduction temperature from 400 to 600 °C, the diffraction intensities decreased obviously, suggesting that high temperature deteriorated the regularity of mesoporous carbon. In comparison with Pt/15AM-T catalysts, obvious decreases in (1 0 0) diffraction intensities were observed for Pt/15AM-SF-T catalysts. The hydro-thermal treatment in aqueous solution of sodium formate during the reduction might cause the collapse of mesopores and changed the structural rigidity of carbon structure.

The wide-angle XRD patterns of the Pt/15AM-T and Pt/15AM-SF-T catalysts (Fig. 1b) displayed four resolved diffraction peaks at $2\theta = 39.8°, 46.3°, 67.4°$ and 81.3°, which can be indexed to the (1 1 1), (2 0 0), (2 2 0), (3 1 1) reflections of face-centered cubic metallic Pt (JCPDS card No. 04-0802). The intensities of diffraction peaks depended on the reduction temperature suggested that high temperature were harmful to the dispersion of Pt particles. Compared to Pt/15AM-T catalysts, a bit stronger diffraction intensities of Pt/15AM-SF-T catalysts were observed. This could be attributed to the removal of chlorine during the aqueous reduction, while the chlorine was considered to inhibit the aggregation of the Pt particles [5].

3.2. N_2 adsorption-desorption

The relevant physico-chemical parameters of Pt/15AM and Pt/Al_2O_3 by nitrogen adsorption-desorption are summarized in Table 1. It is noted that with an increase in reduction temperature, the special surface area and total pore volume of these catalysts increased obviously. This implied that high temperature made the further carbonization of resol composites and the removal of the trace of template. And the extent of carbonization depended on the reduction temperature.

The nitrogen adsorption-desorption isotherms and the Barrett-Joyner-Halenda (BJH) pore size distributions of Pt/15AM-T catalysts and Pt/15AM-SF-T catalysts are shown in Fig. 2. These samples exhibited representative type IV curves with H2 hysteresis loops, which attributed to the presence of well-developed mesopores and micropores [46]. The BJH pore size distribution curves revealed that the mean pore sizes of Pt/15AM-T catalysts were 5.6 nm (Fig. 2a, insert), the same with 15AM [44], while Pt/15AM-SF-T catalysts only obtained mean pore sizes of 4.8 nm (Fig. 2b, insert). Moreover, compared to Pt/15AM-T catalysts, much broader pore size distributions were observed for the Pt/15AM-SF-T catalysts. All these results implied that hydro-thermal treatment during aqueous reduction weakened the structure rigidity of the support, and these results were consistent with the analysis of low-angle XRD patterns (Fig. 1a).

The exact Pt contents of these catalysts measured by ICP-OES are listed in Table 1. With an increase in reduction temperature, the Pt content increase obviously (Table 1, entries 1, 3, 5 and 2, 4, 6, respectively). This also suggested that the mesoporous carbon support was in a dynamic change state during high temperature reduction process. The further carbonization of the resol resulted in the decrease amount of support, and thus Pt content was increased relatively. Pt/15AM-T catalysts had higher Pt contents than Pt/15AM-SF-T catalysts suggested that directly high temperature reduction can inhibit the Pt loss, which always occurred during the aqueous reduction.

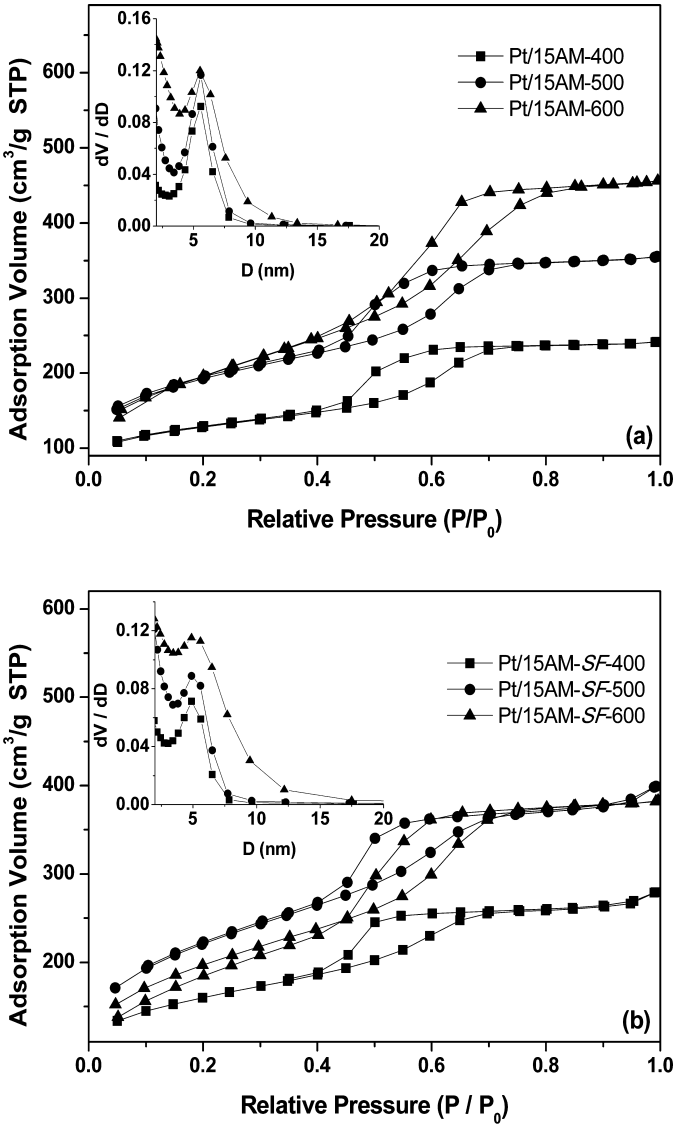

Fig. 2. N_2 adsorption-desorption isotherms: (a) Pt/15AM-T catalysts; (b) Pt/15AM-SF-T catalysts. The insets are the corresponding pore size distribution curves based on the adsorption branch of isotherm.

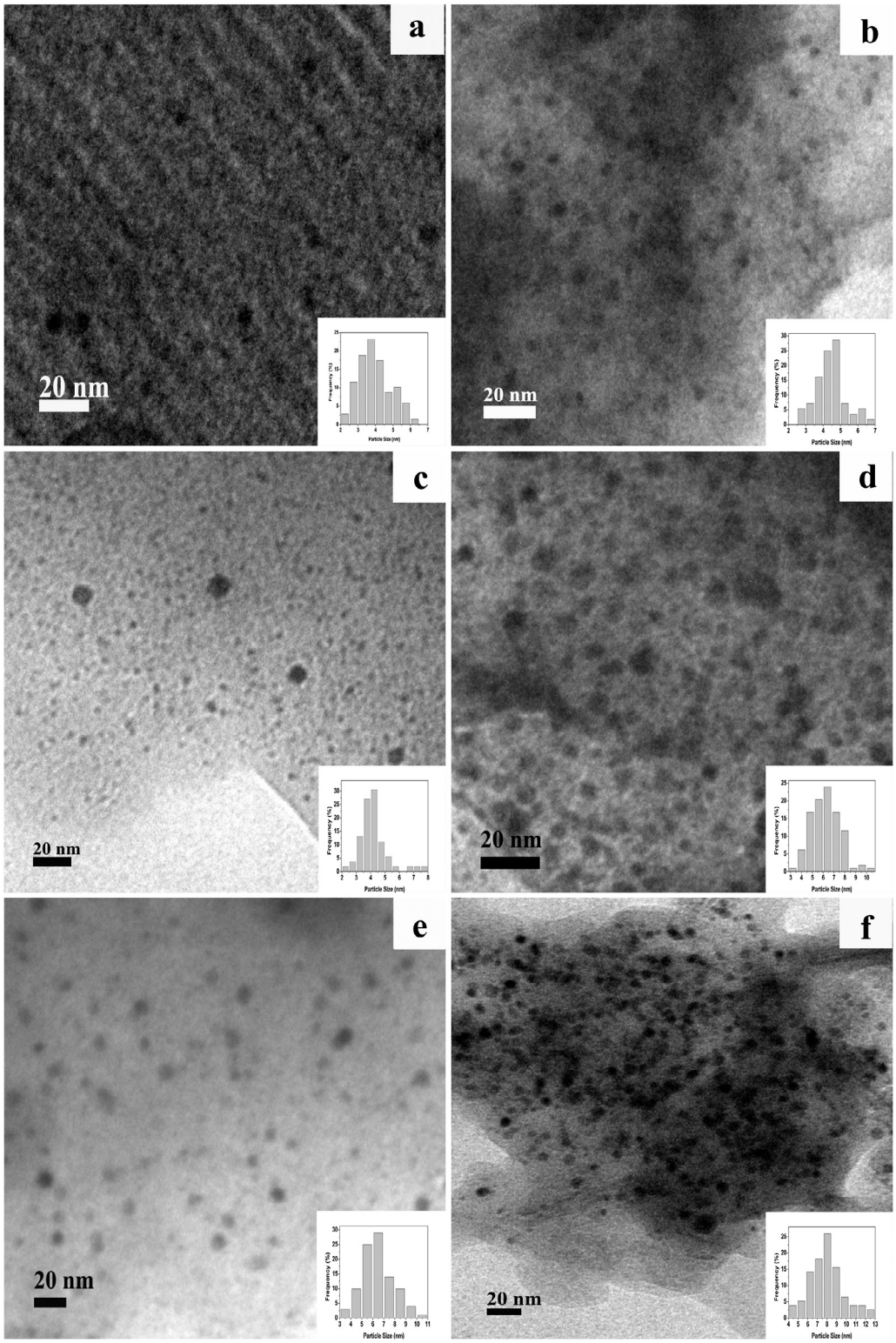

Fig. 3. TEM images of catalysts reduced by different methods. (a) Pt/15AM-400; (b) Pt/15AM-SF-400; (c) Pt/15AM-500; (d) Pt/15AM-SF-500; (e) Pt/15AM-600; (f) Pt/15AM-SF-600. Insets in (a–f) are the corresponding particle size distributions.

3.3. TEM

Fig. 3 displays TEM images of Pt/15AM-T and Pt/15AM-SF-T catalysts. TEM images of Pt/15AM-400 (Fig. 3a) catalyst showed stripe-like and hexagonally arranged pore morphology, confirming mesostructure with 2-D hexagonal pore symmetry [46], while the other catalysts displayed non-visibility hexagonal pore structure. This observation indicated that the loading of Pt precursor and reduction at 400 °C did not destroy the mesostucture of 15AM support, while hydro-thermal treatment or higher temperature may cause the collapse of mesopores. All these results were in good agreement with the low-angle XRD analysis. The particle

Table 2
XPS analysis of various catalysts.

Entry	Catalyst	Cl/Pt	Pt/Al
1	Pt/15AM-600	[a]	0.13
2	Pt/15AM-SF-600	0.44	0.01
3	Pt/15AM-400	0.56	0.09
4	Pt/15AM-SF-400	0.61	0.03
5	Pt/Al_2O_3-600	0.88	–

[a] Below detection limit.

size distribution of Pt/15AM-400 (Fig. 3a, inset) displayed a mean diameter centered at 3.8 nm. When the catalyst reduced at a higher temperature or reduced by aqueous solution of sodium formate, much larger Pt particles could be obtained. This observation was consistent with the wide-angle XRD analysis (Fig. 1b).

3.4. X-ray photoelectron spectra analysis

The chemical species on the catalysts surfaces and their proportions were evaluated by XPS. The C_{1s} peak at 284.6 eV was used for calibration. The Cl/Pt and Pt/Al atomic ratios of the catalysts are summarized in Table 2. It is interesting to observe that the Pt/15AM-600 catalyst had no surface chlorine residues, whereas the Cl/Pt ratios of Pt/15AM-400 and Pt/Al_2O_3-600 were 0.56 and 0.88, respectively. The considerable amount of chorine on the surface of Pt/Al_2O_3-600 also verified the residual chlorine could not totally removed by directly reduction of Pt/Al_2O_3 in hydrogen [35,36,47,48]. The non-chlorine residues on the surface of Pt/15AM-600 could be attributed to the water, which was generated from the further carbonization of alumina–carbon composites. And the water may take away the chlorine, which was originated from the decomposition of Pt precursor during the high temperature reduction. For the Pt/15AM-SF-400 and Pt/15AM-SF-600 catalysts, there were still amount of chlorine left on the surface after reduction by sodium formate solution and washing by deionized water. This must be caused by the hydrophobicity and porous structure of the catalyst support, and the special structural properties barred the water from rinsing the chlorine residuals. The resulting free chlorine attached on the surface of the support was hard to remove by post-treatment in hydrogen. As shown in Fig. 4, the binding energy of $Cl_{2p3/2}$ in Pt/Al_2O_3-600 and Pt/15AM catalysts were about 198.0 eV and 198.8 eV, respectively. The shift binding energy of

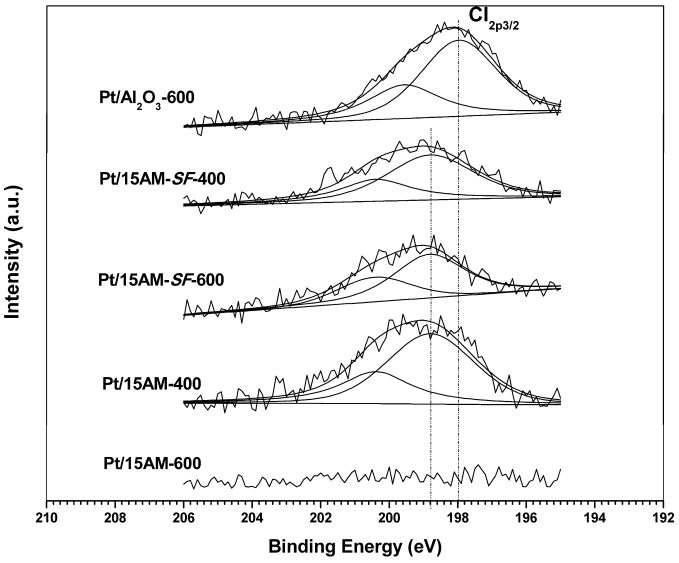

Fig. 4. Cl_{2p} photoelectron spectra of several catalysts.

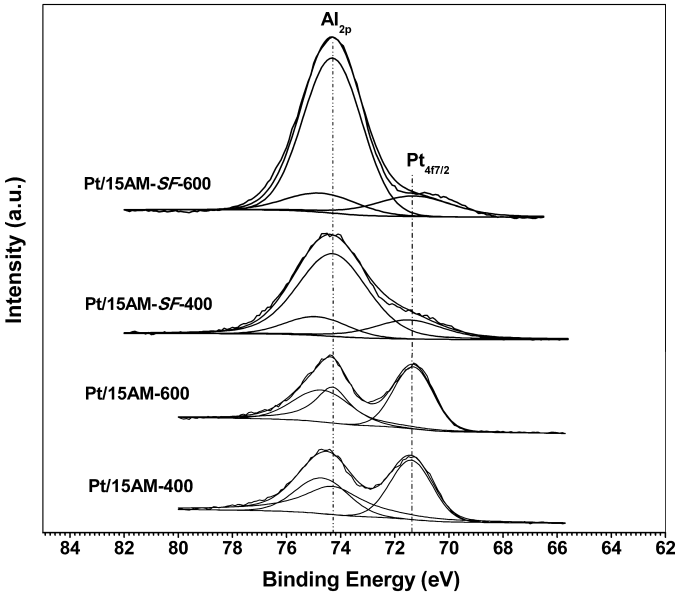

Fig. 5. Pt_{4f} and Al_{2p} photoelectron spectra of Pt/15AM-T and Pt/15AM-SF-T catalysts.

Pt/Al_2O_3 and Pt/15AM catalysts indicated that residual chlorines were more strongly absorbed on the surface of alumina support than on alumina–carbon composites. The residual chlorines on the Pt/Al_2O_3 surface might present as a stable Al–Cl complex [36] or $PtCl_xO_y$ [35], while the chlorines on Pt/15AM catalysts surface probably had a weak interaction with mesoporous carbon, and this weak interaction made the binding energy shifted to a higher value.

Fig. 5 shows the spectra region comprising the Al_{2p} and Pt_{4f} signals of Pt/15AM catalysts. The peak at 74.3 eV (Al_{2p}) could be assigned to Al_2O_3 [49] and the peak at 71.1–71.5 eV ($Pt_{4f7/2}$) was assigned to Pt^0 [50]. The Pt/Al molar ratios of these catalysts were calculated according to fitted spectra and Pt/15AM-600 furnished the highest Pt/Al ratio of 0.13 (Table 2). Compared to Pt/15AM-T catalysts, Pt/15AM-SF-T catalysts obtained much lower Pt/Al ratios. This observation could be attributed to three points: firstly, the hydro-thermal treatment during aqueous reduction destroyed the mesostructure of Pt/15AM-SF-T catalysts (Table 1, Fig. 2b), thus much more alumina exposed to the surface and more platinum particles were masked (Fig. 5); secondly, the aqueous reduction may result in somewhat platinum loss, which was proved by the ICP-OES test (Table 1); thirdly, the aqueous reduced catalysts may have a change in the platinum particles, from plat particles to spherical or hemispherical, resulting in a low Pt/Al ratio [36].

In summary, for our alumina–carbon supported Pt catalysts, one-step 600 °C reduction method avoided the Pt loss and structure deterioration during traditional aqueous reduction. Moreover, one-step reduction procedure saved the extra time without calcination and drying. This simple, effective reduction method can replace the fussy traditional reduction method and also provides an alternative for the preparation of other carbon composites supported metal catalysts.

3.5. Catalytic performance of Pt catalysts with different reduction methods

The conversions and ee values for asymmetric hydrogenation of ethyl pyruvate on CD-modified Pt/15AM-T and Pt/15AM-SF-T are listed in Table 3. It is note that all the catalysts afforded over 96% conversions with the exception of the Pt/15AM-400 catalyst (Table 3, entry 1). With an increase in reduction temperature, the ee value increased obviously (Table 3, entries 1, 3, 5 and entries

Table 3
Effects of catalyst reduction methods on the enantioselective hydrogenation of ethyl pyruvate on CD-modified Pt/15AM and CD-modified Pt/Al_2O_3.[a]

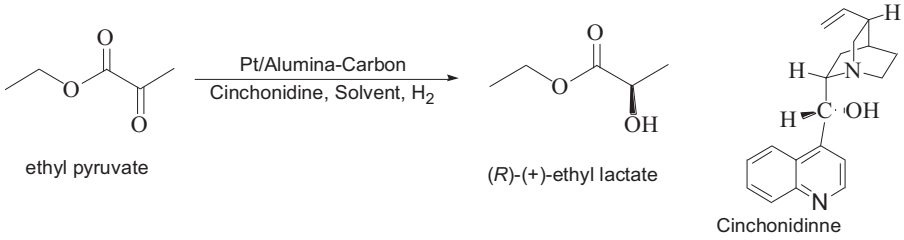

Entry	Sample	Conv.%	ee%
1	Pt/15AM-400	83.9	69.7
2	Pt/15AM-SF-400	96.7	73.4
3	Pt/15AM-500	100	79.0
4	Pt/15AM-SF-500	99.6	80.5
5	Pt/15AM-600	100	87.5
6	Pt/15AM-SF-600	100	82.2
7	Pt/Al_2O_3-600	86.8	67.3
8	Pt/Al_2O_3-SF-400	100	90.4

[a] Reaction conditions: Pt catalyst (100 mg); CD (10 mg); ethyl pyruvate (2 mL); acetic acid (25 mL); H_2 pressure (5 MPa); RT; 1000 rpm; 0.5 h and the main configuration is *R*.

2, 4, 6, respectively) and the Pt/15AM-600 afforded the highest ee value of 87.5% (Table 3, entry 5). These observations could be attributed to the changes of structure properties and surface chemical species by different reduction methods. Firstly, the higher temperature resulted in the further carbonization of the support, which facilitated an increase in exact Pt content relatively (Table 1) and provided more active sites on the surface. Secondly, much more chlorines were taken away by the higher temperature reduction (Table 2) while the chlorines were considered to be poison to active Pt [35]. Thirdly, the further carbonization of carbon composites resulted in an increase relative amount of alumina, which could form a kind of electrophilic alumina compound in acetic acid and provide acidity sites. The alumina compound might be in favor of the adsorption of CD and played an important role in the development of chiral environment [51], and acidity sites linked with the enantioselectivity directly [52]. Pt/15AM-SF-600 catalyst only furnished 82.2% ee value, which was much lower than Pt/15AM-600 catalyst. The poor performance of Pt/15AM-SF-600 catalyst could be attributed to its smaller average pore size (Fig. 2), the slightly aggregation of Pt particles (Fig. 3), the lower surface Pt/Al atomic ratio and the residual chlorine on the surface (Table 2). The former limited the diffusion of CD to Pt surface, the later three gave rise to a decrease in Pt active sites.

Table 4 shows the effects of catalyst reduction methods on the asymmetric hydrogenation of EOPB. It is note that Pt/15AM-600 obtained the highest ee value of 84.8%. And the same tendency with the hydrogenation of ethyl pyruvate is also found: the ee value increased with the reduction temperature of corresponding catalyst. Of particular note is the difference between the asymmetric hydrogenation of ethyl pyruvate and EOPB. In the asymmetric hydrogenation of ethyl pyruvate, Pt/Al_2O_3-SF-400 afforded 90.4% ee value, higher than Pt/15AM-600. However, Pt/15AM-600 obtained a bit higher ee value than Pt/Al_2O_3-SF-400 in the enantioselective hydrogenation of EOPB. This could be explained partly by the large molecular size of EOPB. The Pt/15AM-600 had much larger Pt size than Pt/Al_2O_3-SF-400 and the larger Pt size may beneficial to

Table 4
Effects of catalyst reduction methods on the enantioselective hydrogenation of EOPB on CD-modified Pt/15AM and CD-modified Pt/Al_2O_3.[a]

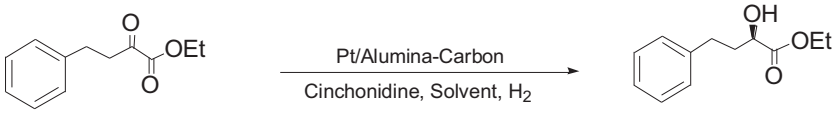

Entry	Sample	Conv.%	ee%
1	Pt/15AM-400	85.9	57.3
2	Pt/15AM-*SF*-400	98.0	57.4
3	Pt/15AM-500	98.2	61.1
4	Pt/15AM-*SF*-500	99.0	65.5
5	Pt/15AM-600	97.0	84.8
6	Pt/15AM-*SF*-600	98.4	75.4
7[b]	Pt/15AM-600	97.4	84.0
8[c]	Pt/15AM-600	95.4	84.9
9	Pt/Al_2O_3-600	98.7	65.3
10	Pt/Al_2O_3-SF-400	98.9	83.5

[a] Reaction conditions: Pt catalyst (100 mg); CD (10 mg); EOPB (1 mL); acetic acid (25 mL); H_2 pressure (5 MPa); RT; 700 rpm; 1 h and the main configuration is *R*.
[b] The amount of Pt catalyst was 50 mg.
[c] EOPB (10 mL), CD (20 mg), acetic acid (50 mL), 2 h.

the co-adsorption of CD and EOPB simultaneously [20]. Ethyl pyruvate had a smaller molecular size, thus the steric hindrance of the diffusion may be not very important, while the surface states of the catalysts may play an important role in determining the catalytic enantioselectivity [29].

From the foregoing, many factors influenced the enantioselectivity for the asymmetric hydrogenation of ethyl pyruvate and EOPB on CD-modified Pt/15AM catalysts. On the surface of the catalyst, Pt content may be the main factor. Pt/15AM-600 catalyst with the highest exact Pt content (6.9 wt%) may result in the highest ee value. However, Li and co-workers [21] had reported that there was no obvious increase in both activity and enantioselectivity when the Pt loading increased from 5 wt% to 10 wt%. And Azmat [53] also had the similar report. Accordingly, we deduced that the Pt content may be a main factor, which influenced the catalytic performance not because of Pt absolute content, but by changing the Pt particle size, morphology and the interaction between Pt particle and the support. 50 mg Pt/15AM-600 catalyst was applied to the asymmetric hydrogenation of EOPB for proving the assumption. It is note that 84.0% ee value (Table 4, entry 7) was obtained on 50 mg catalyst in this reaction system, only slightly lower than 100 mg catalyst. Meanwhile, the reaction system of 10 mL EOPB, 100 mg Pt/15AM-600, 20 mg CD and 50 mL acetic acid also furnished 84.9% ee value (Table 4, entry 8). These observations further confirmed our assumption and indicated that the adsorption of CD on the catalyst surface was irreversible as well [54].

In order to investigate the influence of residual chlorine on enantioselectivity, Pt/Al_2O_3 catalysts were applied for comparisons. Compared to Pt/Al_2O_3-SF-400, Pt/Al_2O_3-600 furnished much lower enantioselectivity, only 67.3% and 65.3% ee values were obtained for the enantioselective hydrogenation of ethyl pyruvate (Table 3, entry 7) and EOPB (Table 4, entry 9), respectively. The physical parameters of Pt/Al_2O_3-600 and Pt/Al_2O_3-SF-400 were very similar (Table 1) except surface chemical species. Pt/Al_2O_3-600 had a high surface chlorine concentration (Table 2), while Pt/Al_2O_3-SF-400 was proved to be no surface chlorine residues [48]. Thus, the low enantioselectivity on Pt/Al_2O_3-600 could be mainly attributed to the surface chlorine residues. Similarly, Pt/15AM-600 had no surface residual chlorine but the other Pt/15AM catalysts all had chlorine residues on the surface. Therefore, we drew the following speculations: One-step reduction method changed pore size, Pt particle size, Pt exact content, surface atomic ratio and surface chlorine residues; all of these factors partly influenced the enantioselectivity of the catalyst in the hydrogenation reaction, but the surface chlorine residue was the critical one.

Besides the catalytic performance, the reusability of heterogeneous catalyst is also a very important matter to consider. Fig. 6 shows the conversions and ee values against the number of runs in the asymmetric hydrogenation of ethyl pyruvate. It was note that Pt/15AM-600 catalyst could be reused for 23 times without distinct loss of activity (Fig. 6a). Since the fresh CD was added to each reaction cycle, the enantioselectivity could maintained over 85% upon 23 times re-use (Fig. 6b). Compared to Pt/15AM-600 catalyst, traditional Pt/Al_2O_3 showed much more inferior reusability, only could be re-used at best six times, which mainly caused by the Pt leaching and the peptization of alumina in acetic acid [20,27,28]. The excellent reusability of Pt/15AM-600 was mainly ascribed to the good stability of the mesoporous carbon structure in acid conditions [55]. Furthermore, Pt particles could be stability by the π-donating from the benzene rings of carbon composites to Pt particles [20]. In addition, one-step 600 °C reduction may result in more facet Pt particles, which had much stronger interaction with the support [56]. These three factors all reduced the Pt loss during each cycle in acetic acid. The excellent reusability of these alumina–carbon composites supported Pt catalysts indicated the possibility of these novel catalysts in industrial application.

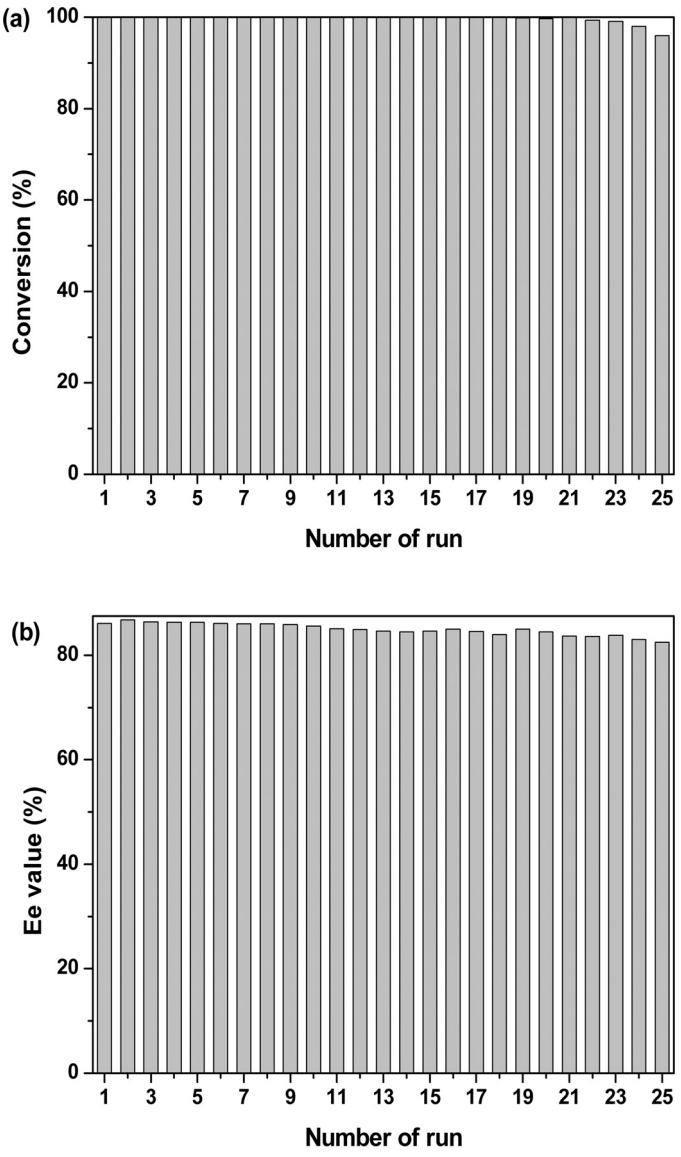

Fig. 6. (A and B) Reusability of Pt/15AM-600 catalyst for the asymmetric hydrogenation of ethyl pyruvate in acetic acid. Reaction conditions: Pt/15AM-600 (100 mg); CD (10 mg); ethyl pyruvate (2 mL); acetic acid (25 mL); H_2 pressure (5 MPa); RT; 1000 rpm; 0.5 h and the main configuration of product is *R*.

4. Conclusion

Pt particles supported on 15% alumina–carbon composites (Pt/15AM) were reduced by liquid phase reduction methods and one-step high temperature methods. The catalyst was reduced by one-step method with hydrogen at 600 °C (Pt/15AM-600) showed superior structure and surface properties: high special surface area, large pore size, high surface Pt/Al atomic ratio and no residual chlorine on the surface. Moreover, CD-modified Pt/15AM-600 catalyst afforded the highest enantioselectivity of 87.5% and 84.8% in the asymmetric hydrogenation of ethyl pyruvate and EOPB, respectively. Of particular note was the reusability of Pt/15AM-600 catalyst, which could be reused for 23 times without distinct loss in catalytic activity in the asymmetric hydrogenation of ethyl pyruvate. This remarkable reusable heterogenous catalyst and the simple, effective one-step reduction in the process of the catalyst preparation may give catalyst workers inspiration on the researches of carbon composites supported catalysts, and provide a potential application in industry.

Acknowledgement

This research was supported by the Natural Science Foundation of Fujian Province, China (Grant No. 2012J05026).

References

[1] M. Bartók, Chem. Rev. 110 (2010) 1663–1705.
[2] Y. Orito, S. Imai, S. Niwa, J. Chem. Soc. Jpn. (1979) 1118–1120.
[3] Y. Orito, S. Imai, S. Niwa, J. Chem. Soc. Jpn. (1980) 670–672.
[4] J.T. Wehrli, A. Baiker, D.M. Monti, H.U. Blaser, J. Mol. Catal. 49 (1989) 195–203.
[5] J.T. Wehrli, A. Baiker, D.M. Monti, H.U. Blaser, J. Mol. Catal. 61 (1990) 207–226.
[6] H.U. Blaser, H.P. Jalett, J. Wiehl, J. Mol. Catal. 68 (1991) 215–222.
[7] H.U. Blaser, H.-P. Jalett, M. Müller, M. Studer, Catal. Today 37 (1997) 441–463.
[8] T. Mallat, S. Frauchiger, P.J. Kooyman, M. Schürch, A. Baiker, Catal. Lett. 63 (1999) 121–126.
[9] C. Exner, A. Pfaltz, M. Studer, H.-U. Blaser, Adv. Synth. Catal. 345 (2003) 1253–1260.
[10] M. Bartók, M. Sutyinszki, K. Balázsik, G. Szöllősi, Catal. Lett. 100 (2005) 161–167.
[11] Z. Liu, X. Li, P. Ying, Z. Feng, C. Li, J. Phys. Chem. C 111 (2006) 823–829.
[12] F. Meemken, N. Maeda, K. Hungerbühler, A. Baiker, Angew. Chem. Int. Ed. 51 (2012) 8212–8216.
[13] N. Maeda, K. Hungerbühler, A. Baiker, J. Am. Chem. Soc. 133 (2011) 19567–19569.
[14] M. Studer, H.U. Blaser, C. Exner, Adv. Synth. Catal. 345 (2003) 45–65.
[15] U. Böhmer, F. Franke, K. Morgenschweis, T. Bieber, W. Reschetilowski, Catal. Today 60 (2000) 167–173.
[16] U. Boehmer, K. Morgenschweis, W. Reschetilowski, Catal. Today 24 (1995) 195–199.
[17] S.P. Griffiths, P. Johnston, P.B. Wells, Appl. Catal. A: Gen. 191 (2000) 193–204.
[18] L. Xing, F. Du, J. Liang, Y. Chen, Q. Zhou, J. Mol. Catal. A: Chem. 276 (2007) 191–196.
[19] S. Basu, M. Mapa, C.S. Gopinath, M. Doble, S. Bhaduri, G.K. Lahiri, J. Catal. 239 (2006) 154–161.
[20] B. Li, X. Li, H. Wang, P. Wu, J. Mol. Catal. A: Chem. 345 (2011) 81–89.
[21] B. Li, X. Li, Y. Ding, P. Wu, Catal. Lett. 142 (2012) 1033–1039.
[22] X. Li, Y. Shen, R. Xing, Y. Liu, H. Wu, M. He, P. Wu, Catal. Lett. 122 (2008) 325–329.
[23] M.J. Beier, J.M. Andanson, T. Mallat, F. Krumeich, A. Baiker, ACS Catal. 2 (2012) 337–340.
[24] Z. Chen, Z. Guan, M. Li, Q. Yang, C. Li, Angew. Chem. Int. Ed. 50 (2011) 4913–4917.
[25] V. Morawsky, U. Prüße, L. Witte, K.D. Vorlop, Catal. Commun. 1 (2000) 15–20.
[26] D.Y. Murzin, P. Mäki-Arvela, E. Toukoniitty, T. Salmi, Catal. Rev. 47 (2005) 175–256.
[27] K. Balázsik, M. Bartók, J. Mol. Catal. A: Chem. 219 (2004) 383–389.
[28] X. Li, Ph D thesis, Chinese Academy of Sciences, 2004.
[29] X.H. Li, X. You, P.L. Ying, J.L. Xiao, C. Li, Top. Catal. 25 (2003) 63–70.
[30] Y. Shen, X. Li, L. Song, H. Wang, P. Wu, Chem. J. Chin. Univ. 30 (2009) 1375–1379.
[31] H. Wang, X. Li, Y. Wang, P. Wu, ChemCatChem 2 (2010) 1303–1311.
[32] H.H. Wang, H.N. Wang, X.H. Li, Y.M. Wang, P. Wu, Chin. J. Catal. 32 (2011) 1677–1684.
[33] S Böttcher, C. Hoffmann, W. Reschetilowksi, DE102011003540A1, Technische Universitaet Dresden, Germany, 2012.
[34] H.S. Oh, J.H. Yang, C.K. Costello, Y.M. Wang, S.R. Bare, H.H. Kung, M.C. Kung, J. Catal. 210 (2002) 375–386.
[35] F.J. Gracia, J.T. Miller, A.J. Kropf, E.E. Wolf, J. Catal. 209 (2002) 341–354.
[36] H. Karhu, A. Kalantar, I.J. Vayrynen, T. Salmi, D.Y. Murzin, Appl. Catal. A: Gen. 247 (2003) 283–294.
[37] X. Li, C. Li, Catal. Lett. 77 (2001) 251–254.
[38] M. Bartók, G. Szöllösi, K. Balázsik, T. Bartók, J. Mol. Catal. A: Chem. 177 (2002) 299–305.
[39] B. Török, K. Balázsik, K. Felföldi, M. Bartók, Ultrason. Sonochem. 8 (2001) 191–200.
[40] B. Török, K. Balázsik, M. Török, G. Szöllösi, M. Bartók, Ultrason. Sonochem. 7 (2000) 151–155.
[41] B. Török, K. Felföldi, G. Szakonyi, M. Bartók, Ultrason. Sonochem. 4 (1997) 301–304.
[42] D. Ferri, T. Bürgi, J. Am. Chem. Soc. 123 (2001) 12074–12084.
[43] W. Chu, R.J. LeBlanc, C.T. Williams, J. Kubota, F. Zaera, J. Phys. Chem. B 107 (2003) 14365–14373.
[44] Q. Li, X. Zhang, M. Xiao, Y. Liu, Catal. Commun. 42 (2013) 68–72.
[45] X. Song, Y. Ding, W. Chen, W. Dong, Y. Pei, J. Zang, L. Yan, Y. Lu, Catal. Commun. 19 (2012) 100–104.
[46] Z. Sun, B. Sun, M. Qiao, J. Wei, Q. Yue, C. Wang, Y. Deng, S. Kaliaguine, D. Zhao, J. Am. Chem. Soc. 134 (2012) 17653–17660.
[47] K. Ito, M. Ohshima, H. Kurokawa, K. Sugiyama, H. Miura, Catal. Commun. 3 (2002) 527–531.
[48] Z. Liu, X. Li, P. Ying, Z. Feng, C. Li, J. Fuel Chem. Tech. 37 (2009) 205–211.
[49] P.M.A. Sherwood, Surf. Sci. Spectra 5 (1998) 1–3.
[50] L. Olsson, E. Fridell, J. Catal. 210 (2002) 340–353.
[51] M. Bartók, K. Balázsik, G. Szollösi, T. Bartók, J. Catal. 205 (2002) 168–176.
[52] S. Böttcher, C. Hoffmann, K. Räuchle, W. Reschetilowski, ChemCatChem 3 (2011) 741–748.
[53] M.U. Azmat, Y. Guo, Y. Guo, Y. Wang, G. Lu, J. Mol. Catal. A: Chem. 336 (2011) 42–50.
[54] I. Bakos, S. Szabó, M. Bartók, E. Kálmán, J. Electroanal. Chem. 532 (2002) 113–119.
[55] R. Xing, N. Liu, Y. Liu, H. Wu, Y. Jiang, L. Chen, M. He, P. Wu, Adv. Funct. Mater. 17 (2007) 2455–2461.
[56] J. Liu, Jimmy, ChemCatChem 3 (2011) 934–948.